# A Study on the Formation of RMF Plasma in the PFRC-2

Gabriel Gonzalez Jusino[1], advised by Professor Sam Cohen[2]
University of Puerto Rico, Rio Piedras[1], Princeton Plasma Physics Laboratory[2]

We describe the effects of seed-plasma parameters on the repeatability of rotating magnetic field (RMF) plasma formation in the PFRC-2. The initial plasma is a steady-state, tenuous ($1\text{x}10^9$ - $1\text{x}10^{11}$ electrons/$\text{cm}^3$) hydrogen plasma, formed by an RF capacitively-coupled external antenna in the source chamber of the device. Previous measurements have shown this relatively low power (2-500 W) plasma may contain a small population of energetic electrons (up to 35 keV), in addition to bulk electrons with temperatures near 5 eV. This 'seed plasma' flows along the main axial magnetic field into the region between the RMF antennas in the central cell. A high power (up to 60 kW), pulsed (up to 300 ms duration), odd-parity RMF at a frequency of 6.042 MHz is then applied to the seed plasma. A higher density (up to $5\text{x}10^{12}$ electrons/$\text{cm}^3$) plasma is formed as a result. Our experiments have studied the effects of varying the seed plasma's parameters on the formation of this RMF plasma. The RMF plasma's breakdown time and the efficiency of power coupling are measured as functions of the initial hydrogen pressure, the main axial magnetic field strength, the RMF antenna power, and the seed plasma RF power. Plasma formation mechanisms are considered.

## Introduction:

The Princeton Field-Reversed Configuration (PFRC-2) is the fourth plasma confinement device designed and built by Dr. Samuel Cohen and his team on their quest to create a high-β, aneutronic, compact fusion reactor. Because of its relatively small size, this device will be very versatile, however, present efforts are focused on two main niche applications. Its cylindrical geometry allows for it to be turned into an unmanned rocket, a space drone of sorts. Unlike Voyager, this rocket would obtain the energy it uses from D-$^3$He fusion, and would eject plasma for thrust, allowing it to cover large distances in a relatively short time. It is also small enough to fit in the back of a supply truck, providing a portable, clean energy source for natural disaster relief or other humanitarian purposes. Another benefit to using smalls reactors, as opposed to a tokamak or a stellarator, is that one could have several of these in series, and the whole plant would not need to shut down to service a single reactor.

The fusion process will take place in the center cell of the device during pulsed intervals in which the odd-parity rotating magnetic field ($RMF_o$) induces an azimuthal current, resulting in closed magnetic field lines which confine a denser, hotter plasma. The PFRC-2 has been very successful in meeting its goals for containment and electron heating, however, to obtain fusion, the current device needs to be scaled up and tuned for ion heating. This is the motivation behind this experiment, to better understand the formation of the RMF plasma with the hopes of improving the device's efficiency.

The PFRC-2:

The device (Figure 1a) consists of three chambers. In the source end cell, the seed plasma is created by a capacitively-coupled helicon antenna (Figure 1c). In the central cell, the plasma is contained in a magnetic bottle created by large axial field coils. This is where the RMF antennas pulse to create an azimuthal electric field (red) which reverses the axial magnetic field lines (green), forming the FRC (Figure 1b).  to further ionize the plasma, and high-temperature superconducting rings conserve the magnetic flux to keep the plasma column from expanding past their diameter of 16cm. The seed plasma then terminates on a floating paddle in the far end cell.

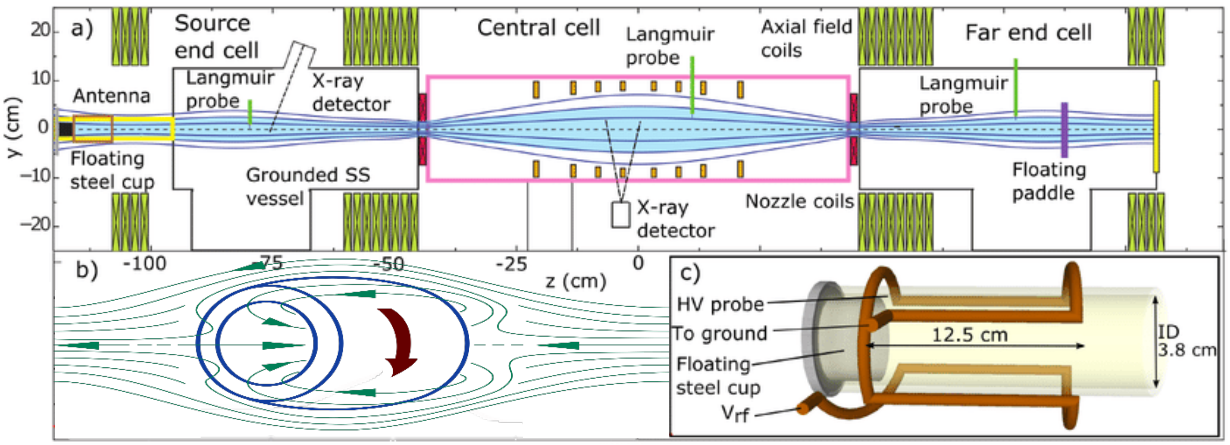


*Figure 1: Simplified Schematic of the PFRC-2*

Method:

The most valuable diagnostics present in the device are non-intrusive, namely spectroscopy and interferometry. This experiment focused on monochrome spectroscopy. Light emitted during each RMF pulse travels through an optic fiber and into a monochromator, which separates visible light and isolates a single wavelength. In this case λ = 486.1nm, which corresponds to Hβ, an aqua light emitted from hydrogen atoms when a bound electron is deexcited from n = 4 to n = 2. The incoming photons are then converted into a current via the photoelectric effect in the photomultiplier tube, and the pre-amplifier then magnifies the signal which is then read as a voltage on the oscilloscope. All measurements are corrected for the preamp delay (1μs) and the RMF antenna trigger delay (25μs).

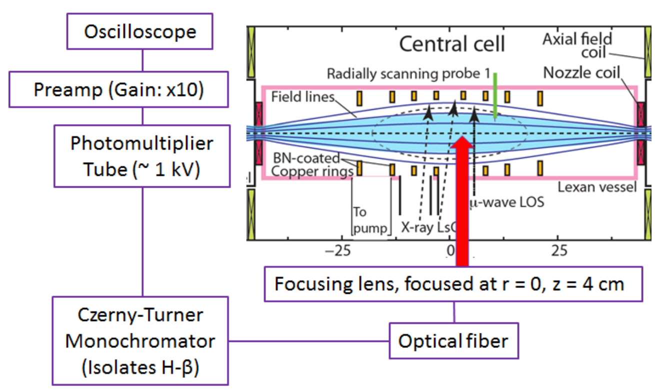


*Figure 2: Monochromator setup*

Seed Plasma:

This steady-state, tenuous ($1x10^9$ - $1x10^{11}$ electrons $cm^{-3}$) hydrogen plasma is colloquially referred to as the seed plasma because it allows the RMF power something to couple to, greatly facilitating the RMF plasma formation. To observe the RMF plasma breakdown, histograms were made by plotting each time the Hβ signal crossed a low voltage threshold. A summary of experimental data (Figure 3) shows that, for steady conditions, the RMF plasma breakdown time decreases rapidly when there is power into the seed plasma antenna. At 0W of power (no seed plasma) the RMF plasma breakdown time is very erratic, thus the large standard deviation shown in the error bar. However, it only changes a total of 15μs after 1.8W. These values for the axial magnetic field ($B_{L-2} = B_a$), initial hydrogen pressure and RMF antenna power are standard for current operations, however, the next generations PFRCs will operate at much higher axial magnetic fields and RMF power.

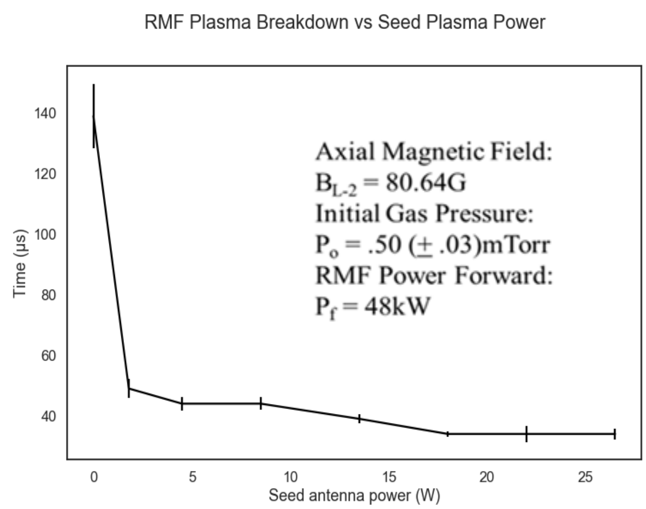


*Figure 3*

Electromechanical issues impeded raising the RMF power without risking the integrity of the equipment, so there are still open-ended questions regarding this trend at high RMF. The experiment continued (Figure 4) by observing the effects of raising the axial magnetic field at three seed plasma powers: 0W, 52W and 110W. The initial hydrogen pressure was set to 0.51mTorr and the RMF power to 47kW consistent with the previous run. Figure 4 shows the RMF breakdown time vs the current through the axial field coils $I_a$, and Figure 3 shows the axial field at the central cell given by

$$B_a \cong 0.72 I_a (G) . \qquad (1)$$

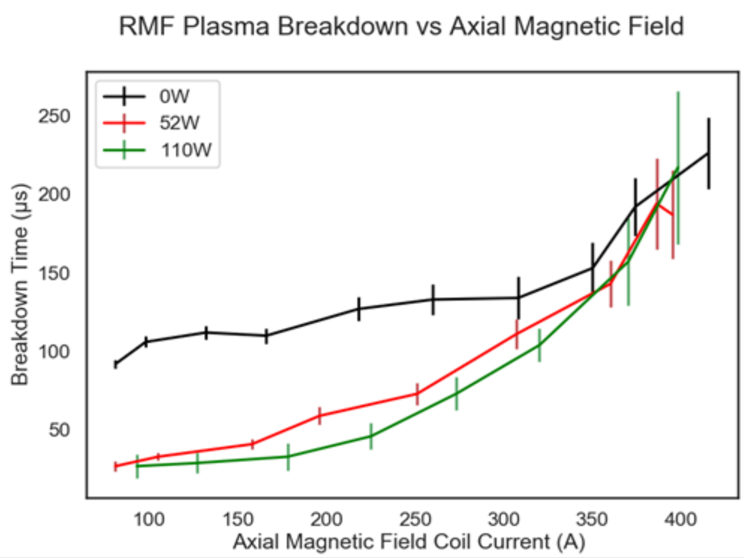


*Figure 4*

The first thing to note is the difference in breakdown times at 0W. This is due to the histogram threshold not being the same, a human error which limits the comparison one can make between the plots, although the trend is still evident. There is a decrease in breakdown times of ~75% at low axial magnetic fields when the seed plasma is turned on with 52W and minimal difference when this power is more than doubled. An unexpected result, though, is that the plots converge at high axial fields. Moreover, the highest seed plasma power became the most erratic at 398A or 286.56G. Although this might not stand true for higher RMF powers, it is clear that high axial magnetic fields dominate the effects of the seed plasma.

Axial Magnetic Field:

The free electrons contained in the center cell between RMF pulses orbit around the axial field lines with a gyrofrequency

$$\omega_{ce} = \frac{eB_a}{m_e c} \text{ (Hz)}. \tag{2}$$

When the RMF antennas turn on, this weaker magnetic field rotates at $\omega_{rmf}$ = 6.042 Hz, inducing an azimuthal electric field $E_\theta \propto \omega_{rmf}$. This is the field that accelerates electrons to create an azimuthal current, which in turn induces another axial magnetic field opposing $B_a$ in the region between the RMF antennas, creating the field-reversed configuration and thus, the denser RMF plasma.

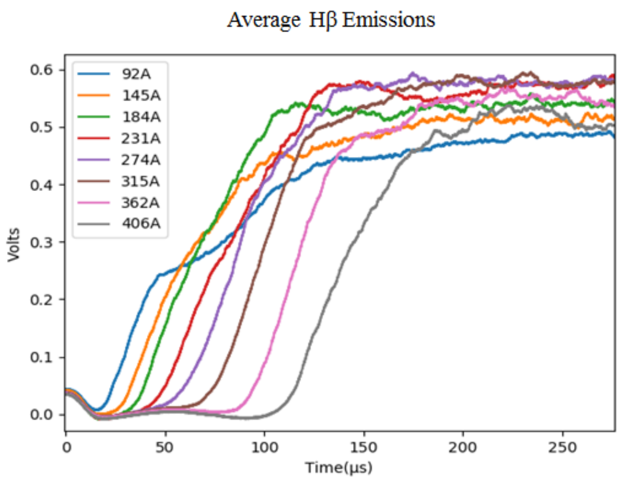


Figure 5

Experimental data shows that the formation of the RMF plasma is delayed by high axial fields. Figure 5 shows a plot of Hβ emissions during the RMF pulse averaged over ~50 pulses at different axial field coil currents. It is clear that the RMF plasma breakdown time increases with the magnitude of the axial magnetic field. This is most likely due to magnetic insulation. As the axial field increases, the electron gyrofrequency increases linearly with it in accordance with equation (2). Since magnetic fields do no work and energy must be conserved, the electron gyroradii decrease as the gyrofrequency increases. When the gyroradii are very small compared to the radial dimensions of the machine (~20 cm diameter), the electrons are turned around as the azimuthal electric field begins to accelerate them. This phenomenon, called magnetic insulation, impedes the electrons from creating an azimuthal current and thus an FRC. This

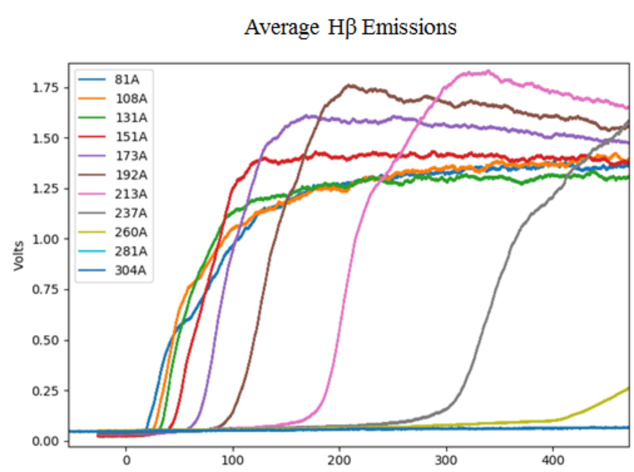


Figure 6

effect lasts a short time until the charge accumulates, and the potential difference gets large enough for the electric force to break the insulation and create a current.

One bothersome question remains unanswered, though. The Hβ emissions at high axial magnetic fields are not only delayed, they are also higher in magnitude by a fair amount. Moreover, it appears that there are some intermediate currents that produce the most emissions (i.e. hotter and/or denser plasma) without being terribly delayed. The experiment was repeated (Figure 6) keeping the RMF antenna power (60kW) and seed plasma power (11-16W) the same and decreasing the initial hydrogen fill pressure from 0.742mTorr to 0.400mTorr. Effectively, the new results showed the RMF plasma breakdown time increased as when the axial magnetic field increased, in agreement with the previous experiment. It can also be seen that the currents that are considered intermediate are not constant but vary with the gas pressure before the pulse. A 231A current at .742mTorr yields high Hβ emissions with a breakdown time t ~ 50μs while a 237A current at .400mTorr results in a breakdown time of t ~ 300μs and emissions that start to die off quicker than for lower currents.

Initial Hydrogen Pressure:

The pressure inside the device changes in numerous ways during and just after the pulse, but we can control the pressure just before each pulse due to the fact that there is at least 1s between pulses. Figure 7 shows the averaged (~50 pulses) Hβ emissions during the beginning of each pulse for an experiment that varied the initial fill pressure while keeping the axial magnetic field at $B_a$ = 74.16G, the seed plasma power at 18W and the RMF antennas at 44.7kW.

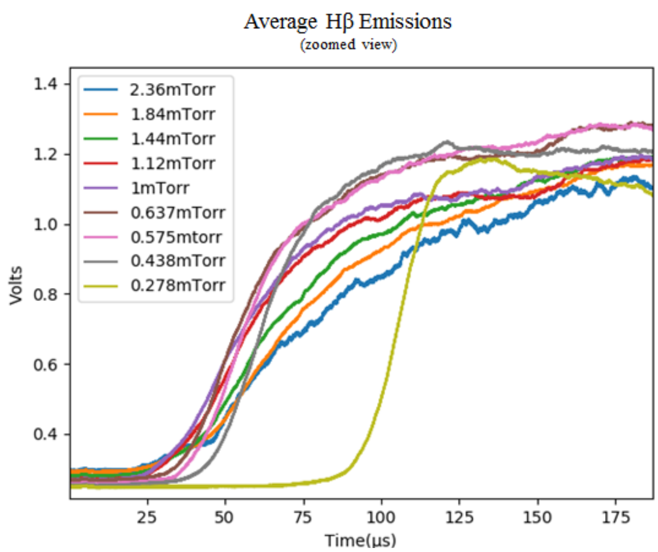


*Figure 7*

High pressures produce the lowest emissions with a gradual slope. As the pressure goes down, the RMF plasma breaks down faster and produces more Hβ light. After the pressure passes 1mTorr, however, the breakdown time increases slightly, but the emissions are still higher once it does break down. At 0.278mTorr, the breakdown time is significantly increased, but the plasma doesn't emit more light than it did at the intermediate pressures.

This gas pressure dependence is most likely due to the collision rates within the plasma. The ionization rate of the seed plasma is given by

$$\frac{\partial n_e}{\partial t} = n_o n_e \langle \sigma v \rangle \tag{3}$$

where $n_e$ is the electron density, $n_o$ is the neutral density and $\langle \sigma v \rangle$ is the velocity averaged cross section which depends on the electron temperature. At high pressures, the electron-neutral collision rate ($n_o\langle\sigma v\rangle$) is high, which keeps the electrons from accumulating much kinetic energy from the azimuthal electric field before transferring it in a collision, so the ionization process is gradual and less energetic. At the lowest pressures, $n_e$ is so low that the electrons gain a large amount of energy before colliding, which results in a significantly delayed but rapid ionization process. At intermediate pressures, say around 1mTorr, the electron-neutral collision rate is such that the electrons are able to gain some kinetic energy but there are still enough electrons to create a chain reaction without delay in the breakdown.

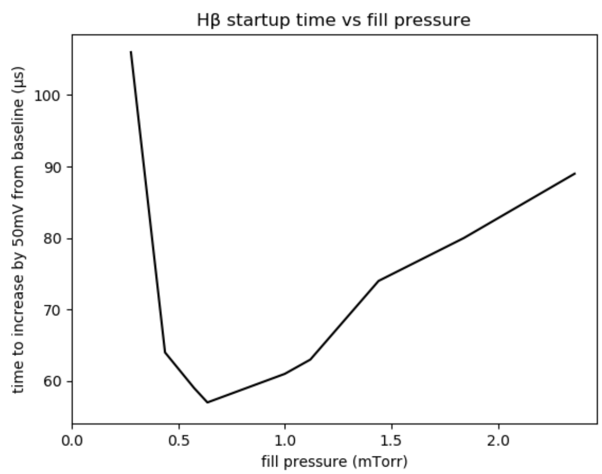


*Figure 8*

Figure 8 shows the time it took each average Hβ signal to increase by 50mV from their respective baseline versus the initial hydrogen pressure for the same experiment as Figure 7. As the previously discussed trend suggested, the RMF plasma's dependence on the initial fill pressure can be thought of as an analogy to Paschen's Law. The lowest pressures require the highest breakdown voltages, there is an intermediate pressure that results in the fastest breakdown, and the breakdown time increases gradually with the pressure after that.

Conclusion:

As expected, at low axial magnetic fields, the seed plasma plays a crucial role in the efficiency of the RMF plasma formation. At high axial magnetic field, the effect of the seed plasma is completely negligible due to the large influence of magnetic insulation. This might be due to the fact that the radial magnetic field is too small compared to the axial field. Additional experimental data taken at higher RMF antenna powers is needed to see whether the seed plasma at high power will reduce the startup time even at such high axial fields.

Magnetic insulation explains the delays in breakdown caused by the axial magnetic field. What it doesn't explain is why the delayed Hβ emissions are higher in intensity. The first thought that comes to mind is the buildup of energy during the insulation, but if that were it, we would expect to see the highest emissions at the highest axial magnetic fields as well as a drop after the initial spike in emissions. This is truly an interesting question that I would someday like to revisit.

One important thing to note about the plots on Figure 7 is that they have different slopes, therefore, Figure 8 would have turned out differently if the time to increase each signal by 100mV was plotted instead of 50mV. This isn't necessarily a bad thing. Similar curves can be plotted for different conditions and eventually one could have a map of what the optimum fill pressures are for given conditions. It could also help provide a target for 'gas puffing' a technique used by the team in which they introduce a quick influx of gas during the pulse that, if timed right, prolongs the stability of the RMF plasma and possibly the FRC.

References:

[1] C. Swanson, P. Jandovitz, S.A. Cohen, Using Poisson-regularized inversion of Bremsstrahlung emission to extract full EEDFs from x-ray pulse-height detector data. (2017) AIP Advaces. 8. 10.1063/1.5019572.

[2] S.A. Cohen, editor; E. Belova, M. Brown, A. Hoffman, T. Intrator, R. Milroy,M. Schaeffer, J. Slough. L. Steinhauer, G. Wurden, and M. Yamada, contributors. (2008)

[3] S.A. Cohen, B. Berlinger, C. Brunkhorst, A. Brooks, N. Ferraro, D.P. Lundberg, A. Roach, and A.H.Glasser, "Formation of collisionless high-βplasmas by odd-parity rotating magnetic fields, Phys.Rev. Lett.98, 145002 (2007)

[4] Hugrass, W., & Grimm, R. (1981). A numerical study of the generation of an azimuthal current in a plasma cylinder using a transverse rotating magnetic field. Journal of Plasma Physics, 26(3), 455-464. doi:10.1017/S0022377800010849

[5] K. Papadopoulos, A. Zigler, D. L. Book, C. Cohen, and D. Hashimshony. "Breakdown of Magnetic Insulation in Semiconductor Plasmas". IEEE Transactions on Plasma Science. vol.24, Issue 3, Jun 1996.